

# Saturation-Induced Instability in Electric Power Systems

Juhua Liu, Bruce H. Krogh and Marija D. Ilić

**Abstract**—This paper concerns the effects of generator controller limits on long-term power system stability. It is shown through an example that when the system operates near its limits, interactions between the speed governor limits and the automatic voltage regulator (AVR) can lead to frequency instability that would not be evident from power-flow analysis or simulations of only the electromechanical dynamics. Analysis of the case study shows that when the generation limit is reached there is an unstable eigenvalue in the system matrix, but we show this observation alone cannot predict whether the instability will occur. We also show that stability can be achieved with the introduction of a power system stabilizer (PSS), which is normally used for transient (fast) stability. This work suggests several directions for further research.

## I. INTRODUCTION

A reliable power grid is vital to the well-being of our society, because we have come to depend on reliable electricity for nearly all aspects of modern life [1]. Power system stability has been recognized as an important problem for secure system operation since the 1920s. Kundur *et al.* classify power system stability into three categories: rotor angle stability (*transient stability*), *frequency stability*, and *voltage stability* [2]. Historically, research has focused on transient stability [3]. As power systems have evolved with larger interconnections and new technologies and controls, it has become important to understand and mitigate conditions that can lead to the other forms of instability. This paper focuses on frequency stability, which is the ability of a power system to maintain steady frequency following a severe system upset, resulting in a significant imbalance between generation and load. In contrast to transient stability, this is a longer-term stability that involves slower phenomena associated with turbine speed control and boiler/reactor protection, with the time frame ranging from tens of seconds to several minutes after severe system upsets.

Due to the increasing demand for electricity and environmental and regulation pressure, today's power systems are more heavily loaded than ever and are often operated near generation, transmission and control limits to maximize the use of existing infrastructure. When saturation in control occurs, the dynamic responsiveness of the system may be severely compromised. Thus, special attention needs to be paid to analyzing and understanding the impact of saturation on the viability of the system. If the limiting condition cannot be alleviated over a period of time, it is possible that one binding constraint will lead to another limit being reached, thus causing a cascading effect that can ultimately result

in system collapse. In this paper, an example is presented in which the post-disturbance steady-state solution exists, but the system becomes unstable and cannot reach the desired post-disturbance equilibrium in some cases due to the saturation in the speed governor control.

The paper is organized as follows. Section II presents the differential-algebraic equations (DAE) model that is used to simulate a two-bus power system. Section III shows the instability in the two-bus power system due to controller saturation. In Section IV we investigate the instability through linearization and eigenvalue analysis. Section V shows that the instability can be eliminated by introducing a power system stabilizer (PSS) to achieve coordination between the governor and AVR. The final section summarizes the paper and discusses directions for future research.

## II. GENERATOR-TRANSMISSION-LOAD MODEL

We study the the two-bus generator-transmission-load system shown in Fig. 1. The system nominal frequency is 50Hz and the system MVA base  $S_{NREF}$  is 400MVA. In general, the dynamic model of power systems is a set of differential-algebraic equations (DAE) of the form [4]:

$$\dot{x} = f(x, y) \quad (1)$$

$$0 = g(x, y), \quad (2)$$

where  $x$  is the vector of dynamic state variables, including the generator flux linkage, rotor angle, shaft speed, and control state variables, and  $y$  is the vector of bus voltages and angles in the power flow constraints. We use the following third-order model for generators with flux linkage  $\lambda_f$ , rotor angle  $\delta$  and shaft speed  $\omega$  as state variables [5]:

$$\begin{aligned} \dot{\lambda}_f &= \frac{\omega_0 r_f}{L_f} \left( \frac{L_{MD}}{L_f} - 1 \right) \lambda_f + \frac{\omega_0 r_f}{L_f} L_{MD} I_d \\ &\quad - \frac{\omega_0 r_f}{M_{dv}} E_{fd} \\ \dot{\delta} &= \omega_0 (\omega - \omega_s) \\ \dot{\omega} &= \frac{P_N}{2HS_{NREF}} T_M + \frac{L_{MD}}{2HL_f} I_q \lambda_f \\ &\quad + \frac{1}{2H} (L_{MD} - M_q) I_d I_q, \end{aligned}$$

where  $E_{fd}$  is field voltage,  $T_M$  is the mechanical torque to the generator shaft,  $I_d$  and  $I_q$  are the currents of  $d$ -axis and  $q$ -axis respectively, and  $\omega_s$  is the system frequency. All these variables are in the per unit system.  $E_{fd}$  is provided by the exciter controlled by the automatic voltage regulator (AVR) and  $T_M$  is provided by the prime mover, a hydroturbine in our case, controlled by a governor. Through the AVR

The authors are with Department of Electrical and Computer Engineering, Carnegie Mellon University, 5000 Forbes Ave., Pittsburgh, PA 15213. Email: {juhual|krogh|ilic}@andrew.cmu.edu

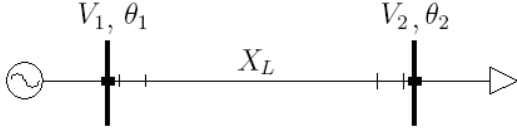


Fig. 1. System configuration.

and governor, the terminal voltage and speed are adjusted automatically. Values for the system parameters and details of the IEEE Type 1 DC exciter and the hydroturbine and its speed governing system used in this example are given in the Appendix.

It is customary to treat frequency dynamics and voltage dynamics separately because the former is more related to generator electromechanics while the latter is more related to electromagnetics. Two reduced-order models are used accordingly. For frequency stability, it is usually assumed that the machine voltage regulator or excitation is strong enough to keep the voltage steady, so the AVR and excitation can be eliminated from the model. For voltage stability, it is assumed that the generator can keep the real power balanced and there is no frequency deviation, so the generator swing equation and governor action can be eliminated from this model. These assumptions may not hold, however, when the generator is operating near full capacity or the excitation limit is reached. Therefore, in our long-term stability study both the AVR and speed governing systems and their physical limits are modeled in detail.

The first algebraic constraints come from the power flow equations [8]. We use the power-balance equations with a constant impedance load model. The transmission line is assumed to be lossless and the load consumes power proportional to the square of its voltage. The other algebraic constraints come from the stator algebraic equations, which relate  $I_d$  and  $I_q$  to the state and network variables as

$$\begin{aligned} 0 &= (L_d + L_{MD})\omega I_d + \frac{L_{MD}}{L_f}\omega\lambda_f \\ &\quad + V_1 \cos(\delta - \theta_1) \\ 0 &= (L_q + M_q)\omega I_q - V_1 \sin(\delta - \theta_1). \end{aligned}$$

Note that the machine internal fluxes are functions of the network frequency [5].

In electric power systems, there are many hard limits due to physical constraints and safety considerations, for example, the limits on the excitation, generator speed, generation, ramp rate, and turbine temperature. Mathematically, there are two types of limits: windup and non-windup [3]. Both types of limits appear in our dynamic model: the control input to the hydroturbine gate position has a windup limit and the AVR excitation has a non-windup limit.

### III. INSTABILITY DUE TO SATURATION

We consider the following scenario. The generator has a capacity of 250MW. The initial load is 200MW and 100MVar. Therefore the generator loading level in terms

TABLE I  
EQUILIBRIUM POINTS.

	Initial equilibrium point	Post-disturbance equilibrium point
$\lambda_f$	-1.1481	-1.1529
$\delta$	0.6138	0.6138
$\omega$	1.0000	0.9919
$E_{fd}$	2.2310	2.4352
$V_R$	0.1348	0.1919
$T_M$	0.8000	0.9628
$V_1$	1.0000	0.9989
$\theta_1$	0.0000	-0.0680
$V_2$	0.9412	0.9377
$\theta_2$	-0.1064	-0.1957

of real power is 80%. Assuming the system is initially at equilibrium, we can solve for all state variables  $x$  and algebraic variables  $y$  from (1) and (2).

The disturbance is a sudden increase of 40MW real power in the load at time  $t = 0s$ . The total load of 240MW equals 96% of the generator capacity. Therefore the generator should be able to serve the load and the values of state and algebraic variables can be calculated. Table I lists the initial and post-disturbance equilibria.

The post-disturbance operating point is acceptable because both system frequency and voltage are kept close to 1 per unit. Also at equilibrium, the AVR and governor are both below their limits. Therefore, if only static power flow analysis is performed, one would conclude that this system can withstand this particular disturbance. We show that this is not necessarily the case, however. When the system is operated near its limits, it is possible that during the transient process, some variables may saturate and thus alter the trajectory and eventually drive the system into instability.

Two cases are studied in this section. First, we observe the system response taking the system from the pre-disturbance equilibrium to the post-disturbance equilibrium when there are no control limits; second, we perform the dynamic simulation with control limits being considered. In Section V the dynamic response is studied when the control limits are taken into account and the AVR is equipped with a PSS. The simulations are performed using the MATLAB DAE solver.

If we remove the hard limit in the governor, allowing the mechanical torque to go over 1 per unit, the system reaches a steady-state equilibrium as shown in Fig. 2. The system is stable and the post-disturbance operating point is acceptable. But the mechanical torque is higher than 1 per unit from 8 sec to 24 sec, which is unrealistic because the gate is beyond its limit. It is thus necessary to see how the system behaves if the hard limit is taken into consideration.

We now consider the simulation of the same scenario with the constraints that the mechanical torque cannot exceed 1 per unit and  $V_R$ , the state variable of AVR, cannot exceed 3.53 per unit. It can be seen from Fig. 3 that at  $t = 8.4s$ , the governor and turbine reach the mechanical torque limit. The mechanical torque is constant at 1 per unit from then on. Due to the lack of mechanical torque, the system frequency

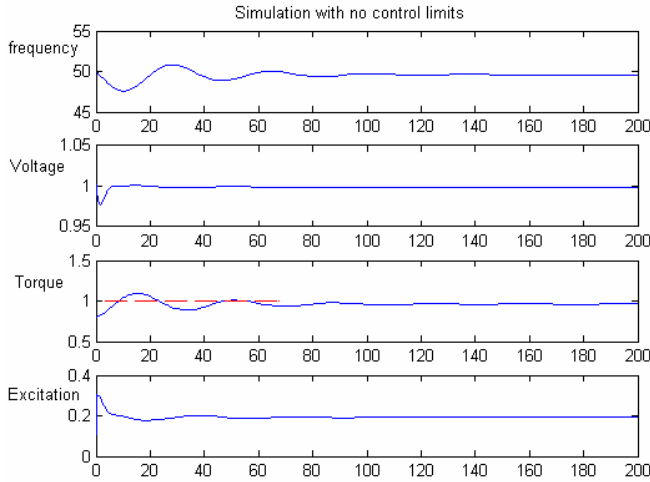


Fig. 2. Simulation without saturation.

continues to decline away from nominal value, though the rate of the decay is slow. Meanwhile the AVR is able to maintain the system voltage steady and close to 1 per unit until  $t = 114.0s$ . At this time, the excitation also reaches its hard limit. Now both controllers are against their limits and thus lose their ability to affect the system. The system voltage and frequency then experience fast decay and finally settle at a very low equilibrium which is outside the acceptable operating limits for the power system. Low frequency tripping would occur long before this equilibrium would be reached.

The existence of such a low final equilibrium is due to the constant impedance load model. If a constant power load model is used instead, the low equilibrium does not exist and the system just diverges after both controller limits are reached. The system is unstable for either load model. This instability phenomenon is perhaps surprising to power engineers because according to the static analysis the post-disturbance equilibrium exists and is acceptable. It is well known, however, that saturation can lead to instabilities.

#### IV. ANALYSIS OF THE CASE STUDY

In this section, we analyze the example in Section III using linearization and eigenvalue analysis. To study the dynamic process, we take snapshots along the trajectory and examine them in detail, similar to the procedure used in [9].

Linearizing the DAE model (1) and (2) about an operating point  $(x_1, y_1)$  gives:

$$\begin{aligned} \Delta \dot{x} &= A\Delta x + B\Delta y + f(x_1, y_1) \\ 0 &= C\Delta x + D\Delta y, \end{aligned} \quad (3)$$

where

$$\begin{aligned} A &= \left. \frac{\partial f}{\partial x} \right|_{x_1, y_1}, & B &= \left. \frac{\partial f}{\partial y} \right|_{x_1, y_1}, \\ C &= \left. \frac{\partial g}{\partial x} \right|_{x_1, y_1}, & D &= \left. \frac{\partial g}{\partial y} \right|_{x_1, y_1}, \end{aligned}$$

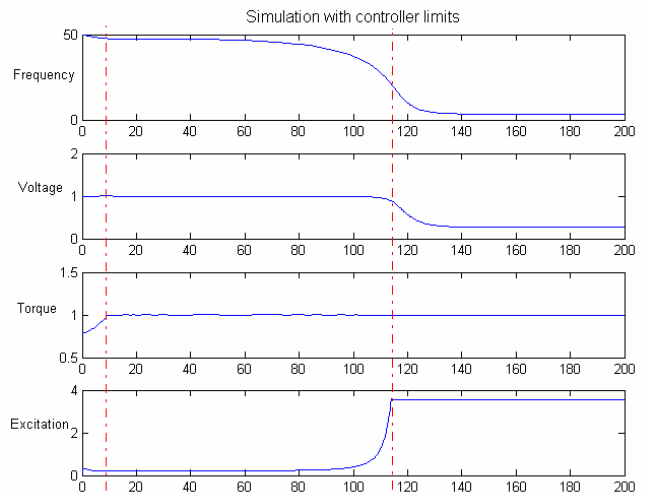


Fig. 3. Simulation with saturation.

and  $f(x_1, y_1)$  is a constant term. If the operating point  $(x_1, y_1)$  is an equilibrium,  $f(x_1, y_1) = 0$ , otherwise it is nonzero.

In our case study the matrix  $D$  is always invertible, so (3) can be transformed to express  $\Delta y$  in terms of  $\Delta x$ . The linearized dynamic model with algebraic constraints being eliminated is then obtained as

$$\Delta \dot{x} = (A - BD^{-1}C) \Delta x + f(x_1, y_1).$$

We define  $A_{sys} = A - BD^{-1}C$  and study its eigenvalues to gain insight into the stability characteristics of the dynamic system. If we are linearizing the system around an equilibrium, then the property of the associated matrix  $A_{sys}$  can tell us if this equilibrium is stable or unstable in the small-signal sense. When we are linearizing the system around points that are not equilibria along the trajectory, we cannot draw similar conclusions with regard to stability just by examining the eigenvalues of the corresponding  $A_{sys}$ . In other words, if at one instant during the transient process we discover that there is one eigenvalue in the right-half plane, we cannot say that the system is necessarily unstable because the notion of stability applies only to equilibrium points. But if we observe the eigenvalues of  $A_{sys}$  for several snapshots, the trend in eigenvalues may give some indication whether or not the system is stable. In Fig. 3, there are two important time points: when the governor reaches its limit and when the AVR is against its limit. We therefore take snapshots at the following points:

- 1)  $t=0-$ , pre-disturbance;
- 2)  $t=0+$ , immediately after the disturbance;
- 3)  $t=8.07$ , before governor reaches limit;
- 4)  $t=8.44$ , after governor reaches limit;
- 5)  $t=113.93$ , before AVR reaches limit;
- 6)  $t=114.01$ , after AVR reaches limit;
- 7)  $t=179.60$ , post-disturbance lower equilibrium.

In addition, also take a snapshot of the post-disturbance equilibrium (called snapshot 8) when the hard limits are

TABLE II  
EIGENVALUES OF  $A_{sys}$ .

Snapshots	1	2	3	4
Eigenvalues	-10.319+10.285i	-10.323+10.288i	-10.394+10.357i	-10.393+10.357i
	-10.319-10.285i	-10.323-10.288i	-10.394-10.357i	-10.393-10.357i
	-2.769	-2.767	-2.768	-2.000
	-1.026	-1.035	-1.031	-1.923
	-1.000	-1.000	-1.000	-1.000
	-0.535+0.618i	-0.514+0.627i	-0.507+0.614i	-0.482+0.605i
	-0.535-0.618i	-0.514-0.627i	-0.507-0.614i	-0.482-0.605i
	-0.034+0.173i	-0.029+0.173i	-0.026+0.172i	-0.026
-0.034-0.173i	-0.029-0.173i	-0.026-0.172i	0.050	
Snapshots	5	6	7	(8)
Eigenvalues	-12.760+12.239i	-5.150	-5.438	-10.370+10.333i
	-12.760-12.239i	-2.000	-2.000	-10.370-10.333i
	-2.000	-1.923	-1.923	-2.767
	-1.923	-1.000	-1.000	-1.034
	-1.000	-1.000	-1.000	-1.000
	-0.501+0.359i	-0.394	-0.769	-0.513+0.622i
	-0.501-0.359i	-0.026	-0.122	-0.513-0.622i
	-0.026	-0.021	-0.026	-0.029+0.173i
0.093	0	0	-0.029-0.173i	

neglected for comparison purposes.

Table II shows the eigenvalues of  $A_{sys}$  evaluated at each snapshot. There is one common zero eigenvalue which is due to the lack of a reference angle. This zero eigenvalue is omitted in the table. We observe that beginning from snapshot 4 ( $t = 8.44s$ ) to snapshot 5 ( $t = 113.93s$ ), there is always one positive real eigenvalue of  $A_{sys}$ . This is due to the effect of the governor saturation.

Participation factor analysis can be used to identify which state variable has the most significant participation in a given mode or eigenvalue [8]. We use this method to identify the state variable associated with the positive real eigenvalue  $\lambda = 0.050$  at snapshot 4. First, the right eigenvector  $v$  and the left eigenvector  $w$  associated with  $\lambda$  are obtained. Then the participation factor  $p_k$  relating the  $k^{th}$  state variable to the given eigenvalue is calculated as

$$p_k = \frac{w_k v_k}{w^T v},$$

where  $w_k$  and  $v_k$  are the  $k^{th}$  components of the left and right eigenvectors, respectively. It can be shown that the sum of all the participation factors associated with a given eigenvalue is equal to 1. The trajectory of the state variable with the largest corresponding participation factor is most influenced by the given eigenvalue. The above participation factor analysis identifies the frequency  $\omega$  as the state variable associated to the positive real eigenvalue  $\lambda = 0.050$ . This indicates that the system is not able to balance the mechanical torque and electrical torque leading to frequency instability.

When the AVR also reaches its limit, there is one zero eigenvalue from snapshot 6 ( $t = 114.01s$ ) to snapshot 7 ( $t = 179.60s$ ). This is because the hard limit of AVR is of non-windup type and  $V_R$  stops acting as a state variable. In other words, the AVR loses its ability to control starting from snapshot 6.

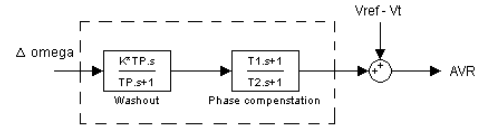


Fig. 4. A power system stabilizer [3].

## V. EFFECTS OF PSS

The AVR and governor in the unstable case in Section III act independently. The AVR responds only to voltage deviations and adjusts the excitation accordingly. The governor reacts only to frequency deviations and adjusts mechanical torque accordingly. When the governor first hits its limit, the system cannot balance the large increase of electrical torque and the frequency decreases. In the meantime, the AVR observes only the voltage deviation, and attempts to increase excitation to maintain a high voltage level, which in fact is bad for the system under this extreme condition because the electrical torque is also kept high indirectly. If by some means, the AVR could know that the governor is experiencing difficulty, then the AVR could help alleviate the situation by temporarily reducing the excitation and thereby reduce the electrical torque. This allows the governor time to recover from the limiting condition and the system would then be stable.

Some generators in electric power systems are equipped with power system stabilizers (PSS). The basic function of a PSS is to improve power system dynamic performance by controlling the excitation system using ancillary stabilizing signals. Commonly used input signals to PSS are generator shaft speed, terminal frequency and power. Figure 4 shows the diagram of PSS using the speed deviation as input with  $K_P = 2.0$ ,  $T_P = 5.0$ ,  $T_1 = 0.3$ ,  $T_2 = 1.0$ . We simulate the unstable case again, except that the AVR is now equipped with PSS. Fig. 5 shows that even though the governor is against its limit for about 30 seconds, with the coordination

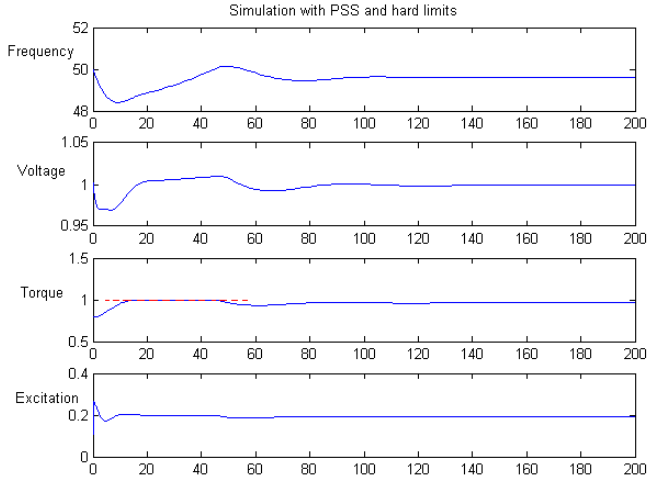


Fig. 5. Simulation with saturation and a PSS.

of AVR and PSS, the system is able to recover the frequency and reach the desired acceptable post-disturbance operating point. A zoom-in of the above three cases in the first 40 seconds of simulation is shown in Fig. 6. We can see that in this time frame, the PSS actually reduces the excitation to help reduce the electrical torque. The transient frequency drop is smaller and it can be recovered later by governor action. Although the voltage drop is slightly larger, it is still within acceptable bounds. This coordination proves to be crucial to preserve the system integrity at the expense of reducing the AVR action immediately after the disturbance.

We take snapshots at the following four instants:

- 1)  $t=12.18$ , before governor reaches limit;
- 2)  $t=13.54$ , after governor reaches limit;
- 3)  $t=42.48$ , before governor becomes unsaturated;
- 4)  $t=44.48$ , after governor becomes unsaturated.

Table III gives the eigenvalues of linearized system matrices  $A_{sys}$  at each point. The eigenvalues all have negative real parts before the governor saturates. From  $t = 13.54s$  to  $t = 42.48s$ , there is a small positive real eigenvalue corresponding to the state variable  $\omega$ . In contrast to the unstable case in Section III, the system returns to an unsaturated condition at  $t = 44.48s$  and the positive real eigenvalue disappears. This shows that the eigenvalue analysis is not sufficient and a more sophisticated method is needed to determine whether or not instability will occur.

## VI. DISCUSSION

As today's power systems are operated closer to physical and control limits, traditional static load flow analysis and simulation of reduced-order models may be inadequate to determine whether or not a system will operate safely when subjected to disturbances. As shown in this paper, even if the static solution exists for the post-disturbance conditions, it is still possible for the system to lose stability when constraints are taken into account. The examples in this paper also illustrate that eigenvalue analysis alone is inadequate for predicating instability.

The instability observed in the example in this paper is caused by a saturation constraint. We are currently investigating the application of hybrid system techniques to determine conditions for stability and instability in power systems [10], [11]. Methods for designing controllers that will improve stability even when saturation occurs, such as the introduction of a PSS as discussed in Section V, are also of interest. One approach for designing controllers that deal with generator limits has been proposed in [12].

## APPENDIX

The generator parameters used in our paper are:

$$\begin{aligned} r_f &= 0.0011 & L_{MD} &= 0.203 & L_d &= 0.219 \\ L_q &= 0.219 & L_f &= 0.2222 & M_{dv} &= 2.351 \\ M_q &= 2.351 & T_{d0} &= 7.695 & H &= 6.3 \\ P_N &= 250MW \end{aligned}$$

The block diagram of AVR and associated parameters are:

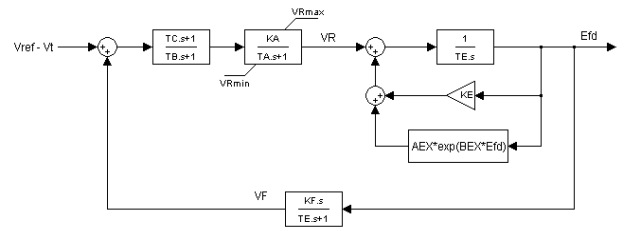


Fig. 7. IEEE Type 1 DC exciter/AVR [6].

$$\begin{aligned} A_{EX} &= 0.0033 & B_{EX} &= 1.303 & K_A &= 50 \\ K_E &= 0 & K_F &= 0.2 & T_A &= 0.05 \\ T_B &= 1.0 & T_C &= 1.0 & T_E &= 1.0 \\ T_F &= 1.0 & V_{RMax} &= 3.53 \end{aligned}$$

The block diagram of turbine and governor and associated parameters are:

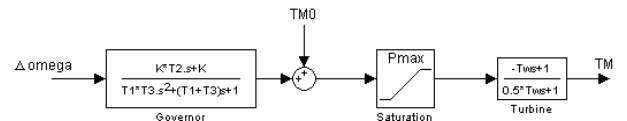


Fig. 8. Hydroturbine and governor [7].

$$\begin{aligned} K &= 20 & T_1 &= 38.48 & T_2 &= 5.0 \\ T_3 &= 0.52 & T_W &= 1.0 & P_{Max} &= 1.0 \end{aligned}$$

## ACKNOWLEDGMENTS

This research was supported by National Science Foundation (NSF) Information Technology Research (ITR) program, contract no. CNS-0428404.

## REFERENCES

- [1] U.S.-Canada Power System Outage Task Force, "Final Report on the August 14, 2003 Blackout in the United States and Canada: Causes and Recommendations", April 2004.
- [2] P. Kundur et al., "Definition and Classification of Power System Stability", *IEEE Transactions on Power Systems*, Vol. 19, No. 2, pp. 1387-1410, May 2004.
- [3] P. Kundur, *Power System Stability and Control*, McGraw-Hill, New York, 1994.

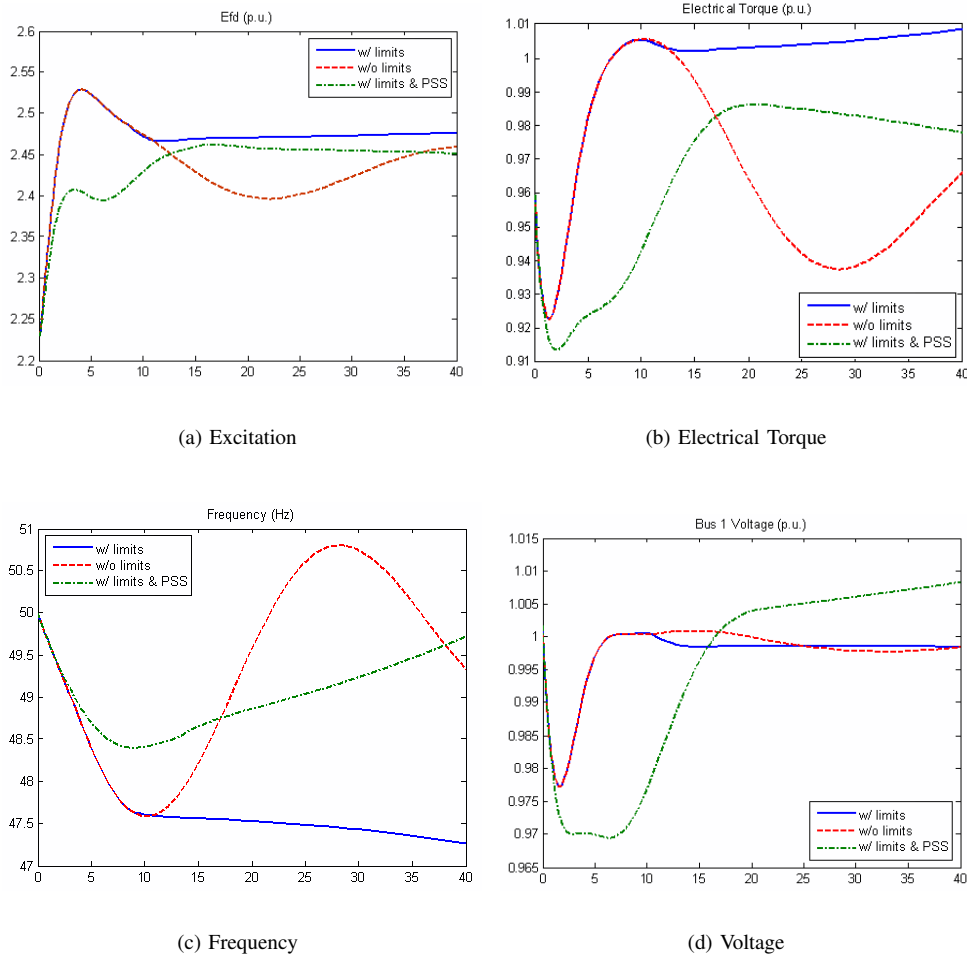


Fig. 6. Comparison of three cases in the first 40s.

TABLE III  
EIGENVALUES OF  $A_{sys}$  (WITH PSS).

Snapshots	t = 12.18 s	t = 13.54 s	t = 42.48 s	t = 44.48 s
Eigenvalues	-10.380+10.343i	-10.382+10.344i	-10.374+10.336i	-10.373+10.335i
	-10.380-10.343i	-10.382-10.344i	-10.374-10.336i	-10.373-10.335i
	-2.768	-2.000	-2.000	-2.768
	-1.000	-1.923	-1.923	-1.000
	-1.000	-1.000	-1.000	-1.000
	-0.870	-1.000	-1.000	-0.858
	-0.721	-0.447	-0.446	-0.735
	-0.308+0.592i	-0.350+0.603i	-0.359+0.607i	-0.317+0.595i
	-0.308-0.592i	-0.350-0.603i	-0.359-0.607i	-0.317-0.595i
	-0.047+0.111i	-0.026	-0.026	-0.047+0.111i
-0.047-0.111i	0.027	0.026	-0.047-0.111i	

[4] M. D. Ilić, J. Zaborszky, *Dynamics and Control of Large Electric Power Systems*, John Wiley & Sons, New York, 2000.

[5] Tractebel and Electricité de France, *EUROSTAG User's Manual Release 4.2*, October 2002.

[6] Tractebel and Electricité de France, *EUROSTAG Tutorial*, October 2002.

[7] IEEE Committee Report, "Dynamic models for steam and hydro turbines in power systems study", *IEEE Transactions on Power Apparatus Syst.* 1904-1915, 1973.

[8] P. W. Sauer and M. A. Pai, *Power System Dynamics and Stability*. Prentice Hall, Upper Saddle River, New Jersey, 1998.

[9] G. K. Morison, B. Gao, P. Kundur, "Voltage Stability Analysis Using Static and Dynamic Approaches", *IEEE Transactions on Power Systems*, Vol. 8, No. 3, pp. 1159-1165, August 1993.

[10] R. A. Decarlo, M. S. Branicky, S. Pettersson and B. Lennartson "Perspectives and results on the stability and stabilizability of hybrid systems", *Proceedings of the IEEE*, Vol. 88, No. 7, pp. 1069 - 1082, July 2000.

[11] Mikael Johansson, *Piecewise Linear Control Systems*, Springer-Verlag Berlin Heidelberg, 2003.

[12] Takao Watanabe, "Robust decentralized turbine-governor control subject to saturation nonlinearity", *Proceedings of the American Control Conference*, Vol. 3, pp. 1948-1953, May 2002.